Journal of
Materials Chemistry C

Materials for optical, magnetic and electronic devices

Accepted Manuscript

This article can be cited before page numbers have been issued, to do this please use: X. Liang, W. Huang, Q. Lu, R. Gao, M. Li, Z. Zhuo, M. Ni, N. Sun, L. Sun, X. An, Y. Han, J. Lin and L. Bai, *J. Mater. Chem. C*, 2025, DOI: 10.1039/D5TC02016F.

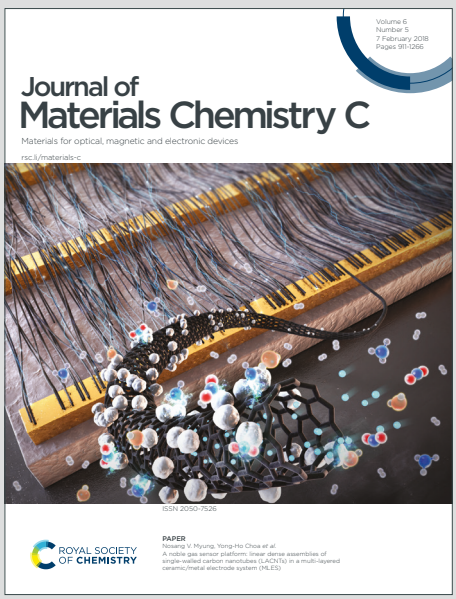

ROYAL SOCIETY OF CHEMISTRY

rsc.li/materials-c

View Article Online
DOI: 10.1039/D5TC02016F

ARTICLE

Balancing the Mechanical and Optoelectronic Properties of Light-Emitting Copolymers via Precise Control of Soft-to-Rigid Segment Ratio

Received 00th January 20xx,
Accepted 00th January 20xx

DOI: 10.1039/x0xx00000x

Xinyu Liang,‡[a] Wenxin Huang,‡[a] Qingqing Lu,‡[a] Rui Gao,[a] Mengyuan Li,[a] Zhiqiang Zhuo,[a] Mingjian Ni,[b] Ning Sun,[a] Lili Sun,[c] Xiang An,[a] Yamin Han,[a] Jinyi Lin[a] and Lubing Bai*[a]

Light-emitting polymers with tunable mechanical properties are desirable for flexible optoelectronic devices. Herein, adopting the synthetic routes for polyurethanes (PU), we successfully developed a series of blue light-emitting copolymers by incorporating diarylfluorene-based trimer (rigid segment) and polydimethylsiloxane (PDMS) (soft segment) with precisely tunable mechanical properties from brittleness to viscoelasticity. The impact of varied soft-to-rigid ratio on the balance of mechanical and optoelectronic properties was thoroughly investigated combining thermodynamic analysis, tensile testing of free-standing films and solution-processed polymer light-emitting diodes (PLEDs). These copolymers maintained efficient deep-blue emission regardless of segment ratio, and PLEDs based on these copolymers (content of PDMS < 30%) also exhibited comparable performances with a turn-on voltage of ~4 V. This study highlights the importance of achieving the optimal balance between mechanical and optoelectronic properties in materials design, providing critical insights for developing flexible optoelectronic polymers.

Introduction

Stretchable light-emitting devices have garnered substantial attention owing to their potential applications in next-generation wearable electronics and flexible displays.[1-3] Unlike the conventional structural engineering such as island-bridge, buckling or textile structures,[4] polymer-based intrinsically stretchable light-emitting diodes offer unique advantages for applications that require both mechanical flexibility and stable optoelectronic performance.[5] Approaches for regulating the mechanical properties of light-emitting conjugated polymers from brittleness to viscoelasticity, including side-chain and backbone engineering, have attracted much attention in recent years.[6-10] Among these approaches, the construction of block copolymers incorporating non-conjugated elastic polymers has demonstrated significant potential for simultaneously enhancing mechanical toughness while introducing novel functionalities.[11-15] However, since the optoelectronic properties of semiconducting polymers are predominantly governed by the π-conjugated moiety stacking, the incorporation of insulating non-conjugated elastomers would inevitably compromise charge transport mobility and ultimately degrade device performance.[6,17] Thus, achieving an optimal balance between mechanical and optoelectronic properties in these block copolymers is necessary for advancing stretchable light-emitting devices.

Indeed, the enhancement of fracture strain achieved through side-chain or backbone engineering of conjugated polymers is inherently limited. To address this, constructing composite semiconducting polymer films by blending with thermoplastic elastomers (TPEs), such as polyurethane (PU) and polyolefin (PO), has been extensively explored in stretchable organic light-emitting diode (OLED),[18,19] organic field-effect transistor (OFET)[20-22] and organic photovoltaic (OPV).[23,24] However, for polydimethylsiloxane (PDMS), an elastomer renowned for its exceptional stretchability, optical transparency and thermal stability,[25] the large Flory-Huggins interaction parameter (χ = 4.04 K) between it and conjugated polymers always leads to significant phase separation inside composite films,[19] which has deleterious effects on the optoelectronic performances. Previous studies about PDMS-based copolymers has predominantly focused on their mechanical properties for applications as the substrate of flexible electronics. Recently, incorporating π-conjugated rigid components into elastic polymers by controlling the ratio of soft-to-rigid segments in polymer chains has emerged as a promising approach to develop stretchable light-emitting polymers.[14,26] In this context, investigating PDMS-based block copolymers with systematically varied segment ratios is

[a] State Key Laboratory of Flexible Electronics (LoFE) & Institute of Advanced Materials (IAM), School of Flexible Electronics (Future Technologies), Nanjing Tech University (NanjingTech), Nanjing 211816, China.
Email: iamlbbai@njtech.edu.cn
[b] The Institute of Flexible Electronics (IFE, Future Technologies), Xiamen University, Xiamen, 361005, China.
[c] School of Flexible Electronics (SoFE) & State Key Laboratory of Optoelectronic Materials and Technologies, Sun Yat-sen University, Shenzhen, 518107,China.
† Electronic Supplementary Information (ESI) available: Synthetic procedures, experimental details, and supplemental figures. See DOI: 10.1039/x0xx00000x
‡ These authors contributed equally.

View Article Online DOI: 10.1039/D5TC02016B

meaningful for elucidating the fundamental structure-property relationship in this novel kind of optoelectronic copolymers.

In this work, by adopting a synthesis procedure compatible with scalable manufacturing, we designed a series of PUTrF-co-PDMS copolymers with tunable mechanical properties by varying the ratio between rigid (diarylfluorene trimer, a high-efficiency blue emitter) and soft (PDMS) segments. The influence of copolymerization ratio on the thermodynamic, mechanical, and optoelectronic properties of these copolymers was systematically investigated. Furthermore, the solution processability and performance characteristics of polymer light-emitting diodes (PLEDs) fabricated from these polymers were comprehensively evaluated. This comprehensive study elucidates the fundamental structure-property relationship while simultaneously advances the development of high-performance light-emitting polymers tailored for stretchable displays.

Results and discussion

Preparation and structural characterization

Firstly, a diarylfluorene-based trimer (TrF-OH) with terminal hydroxyl groups was synthesized, and mixed with hydroxyl-terminated polydimethylsiloxane (PDMS-OH, Catalog No. 481246) in different molar ratios. Then, the mixtures were reacted with 1,6-hexamethylene diisocyanate (HDI) to yield the target copolymers, PUTrF-co-PDMS, which were respectively designated as PUTrF, PUTrF-10-PDMS, PUTrF-30-PDMS, and PUTrF-50-PDMS, according to their rigid-to-soft segment ratios (x:y = 10:0, 9:1, 7:3, 5:5) (Figure 1a). The detailed synthesis procedure is described in the Supplementary Information (Schemes S1). All materials involved in the synthetic routes were characterized and confirmed by ^{1}H-NMR, ^{13}C-NMR, and mass spectrometry, respectively (Figures S1-S7). The calculated incorporation ratios of PDMS in the copolymers are consistent with the theoretical ratios (Table S1). The number-average molecular weight (M_n) and polydispersity index (PDI) of these copolymers were measured by gel permeation chromatography (GPC) with tetrahydrofuran (THF) as the eluent (Table S1). As shown in Figure 1b, these copolymers exhibit distinct morphological variations dependent on PDMS content at room temperature. It's obvious that, the physical state of PUTrF is a hard and brittle bulk powder. When the ratio of PDMS increases from 10% to 30%, the copolymers become more softer while maintaining solid-state. Notably, PUTrF-50-PDMS exhibits a cream-like viscous state at ambient temperature, demonstrating the effectiveness of incorporating soft segment in modulating the polymer mechanical properties.

Interchain hydrogen bonding interactions

To further verify the successful incorporation of PDMS segment, Fourier-transform infrared spectroscopy (FT-IR) analysis was

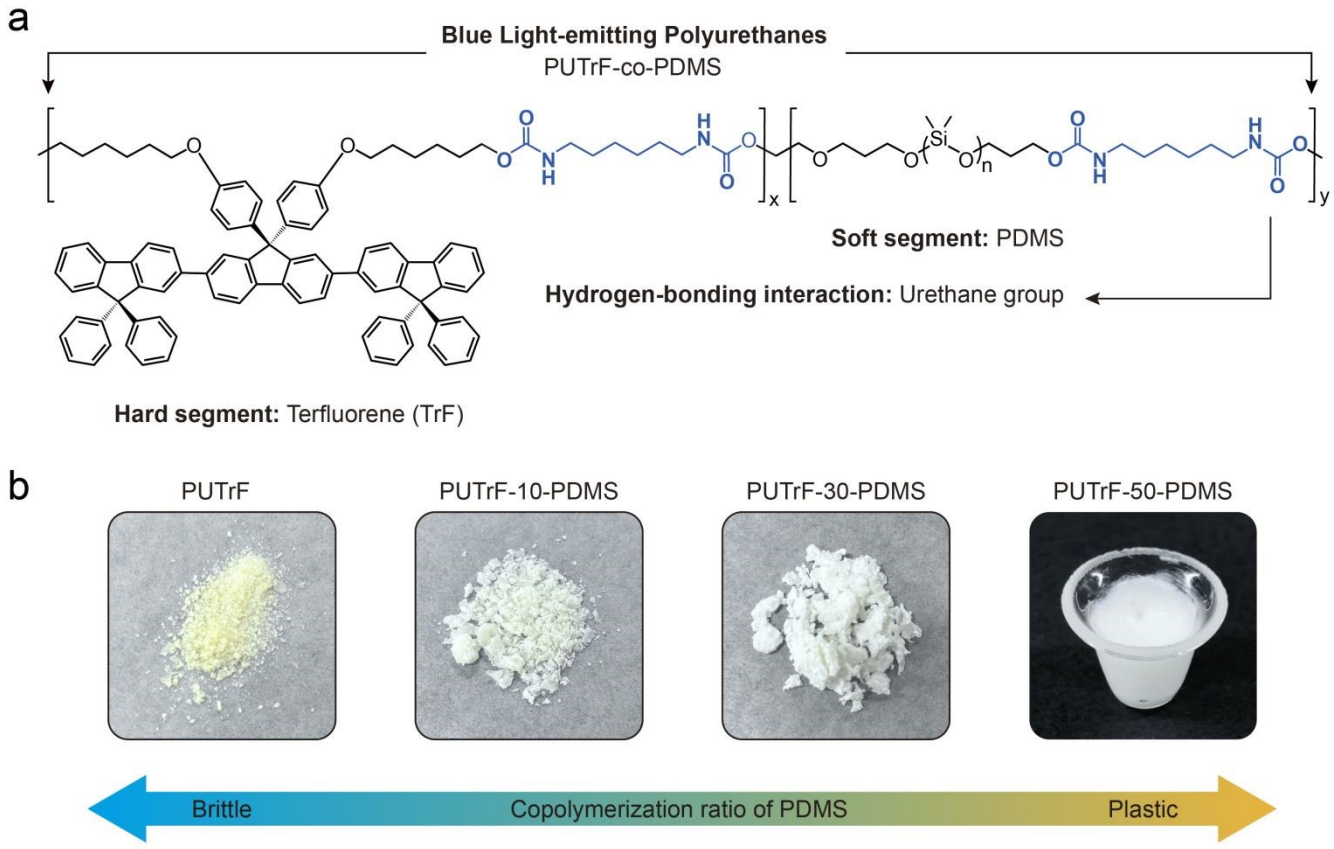

Fig. 1 (a) Design of the chemical structure of PUTrF-co-PDMS. (b) The photographs of copolymers at room temperature with PDMS ratio of 0%, 10%, 30% and 50%, named as PUTrF, PUTrF-10-PDMS, PUTrF-30-PDMS and PUTrF-50-PDMS, respectively.

View Article Online
DOI: 10.1039/D5TC02016F

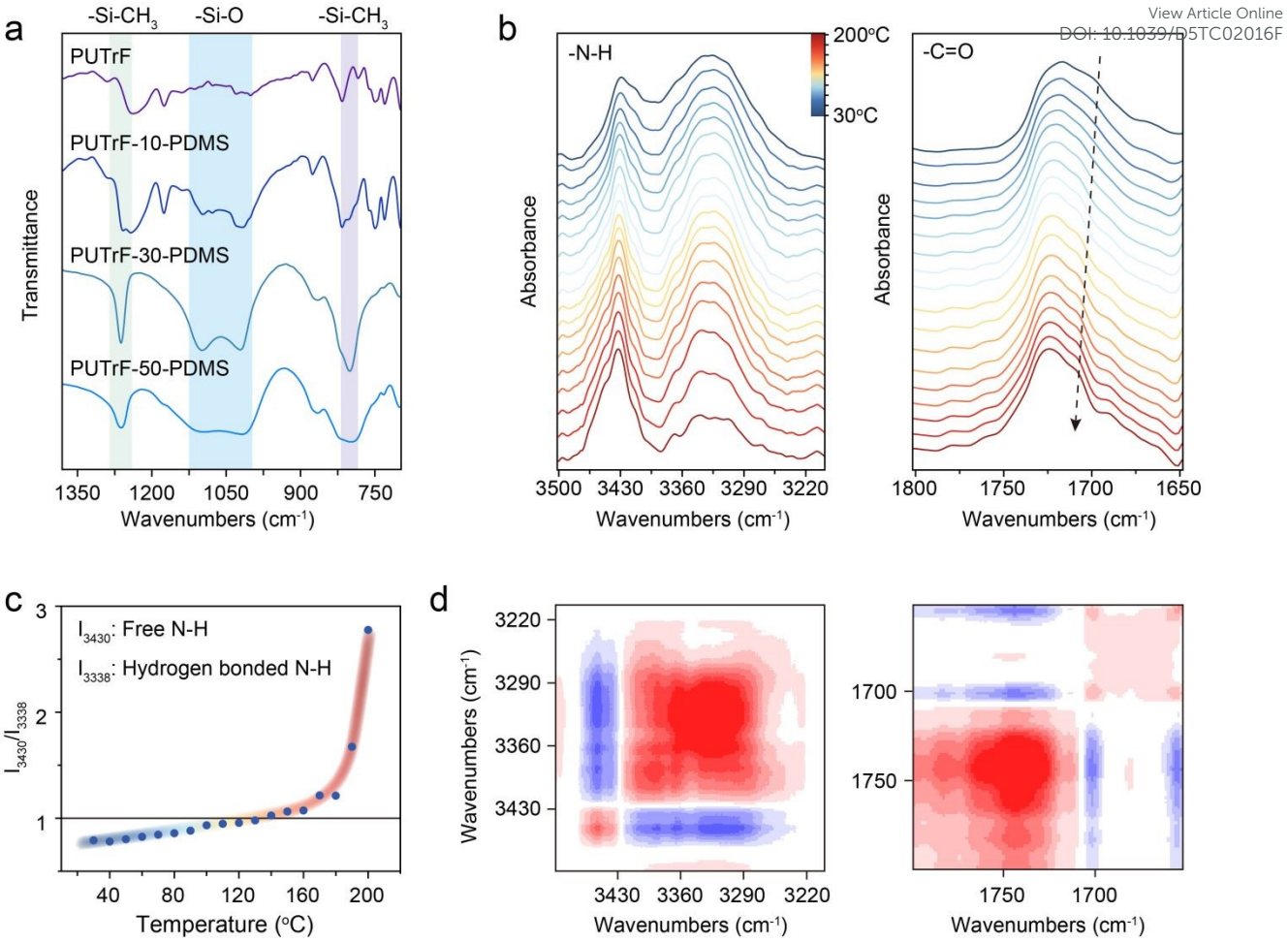

Fig. 2 Characterization of interchain hydrogen bonding interactions. (a) Fourier transform infrared (FT-IR) spectra of these copolymers. (b) Temperature-dependent FT-IR spectra of PUTrF with temperature from 30°C to 200°C, with an interval of 10°C. (c) The ratio variation in characteristic peak intensity of free N-H bonds to hydrogen-bonded N-H bonds. (d) 2D-COS synchronous spectra of N-H stretching vibration peak (left) and C=O stretching vibration peak (right), which generated from temperature-dependent FT-IR.

performed on these copolymers. As shown in Figure 2a, the characteristic peak of Si-CH_3 stretching vibration at around 1260 cm^{-1} and Si-CH_3 bending vibration at around 800 cm^{-1}, as well as the Si-O-Si asymmetric stretching vibration at 1000-1100 cm^{-1} became more prominent with increasing PDMS content, confirming the successful incorporation of soft segments in these copolymers. Significantly, as a new type of polyurethane, these copolymers contain urethane groups that capable of forming interchain hydrogen bonds. Thus, in order to confirm this non-covalent interaction, temperature-dependent FT-IR measurement was conducted on the representative polymer-PUTrF. Figure 2b reveals the temperature-dependent spectral shifts of the stretching vibrations of N-H at 3500-3200 cm^{-1} and C=O at 1680-1800 cm^{-1} across the temperature range of 30 to 200°C. As the temperature increases, we observed that the intensity at 3338 cm^{-1} corresponding to bonded N-H decreases, while the intensity at 3430 cm^{-1} corresponding to free N-H increases. The ratio variation shown in Figure 2c clearly reveals this trend. Meanwhile, the characteristic peak of bonded C=O at 1700 cm^{-1} exhibited an intensity reduction and a 10 cm^{-1} blue shift. These observations clearly demonstrate the thermal dissociation of interchain hydrogen bonds between urethane groups. Furthermore, Two-dimensional correlation spectroscopy (2D-COS) analysis of the N-H and C=O vibrational regions was performed (Figure 2d), revealing strong spectral correlations in these characteristic peaks. As we know, constructing dynamic non-covalent interactions, particularly hydrogen bonding, within flexible polymer chains represents an significant approach for enabling internal energy dissipation upon strain.[27] Therefore, we speculate that the internal plasticizing effect of PDMS soft segments and the interchain weak interactions will have a synergistic effect on the polymer's mechanical properties.

Thermodynamics, mechanics, and rheological testing

Thermogravimetric analysis (TGA) and differential scanning calorimetry (DSC) were conducted to characterize the thermal properties of these copolymers in detail (Figures S8 and S9). Figure 3a shows the variation of decomposition temperature (T_d) and glass transition temperature (T_g) of PUTrF-co-PDMS copolymer with increasing content of soft segment. All these copolymers exhibited appreciated thermal stability, with T_d remaining above 300°C, while exhibiting a substantial decrease in T_g from 147°C to 5°C with the increased proportion of PDMS.

View Article Online
DOI: 10.1039/D5TC02016F

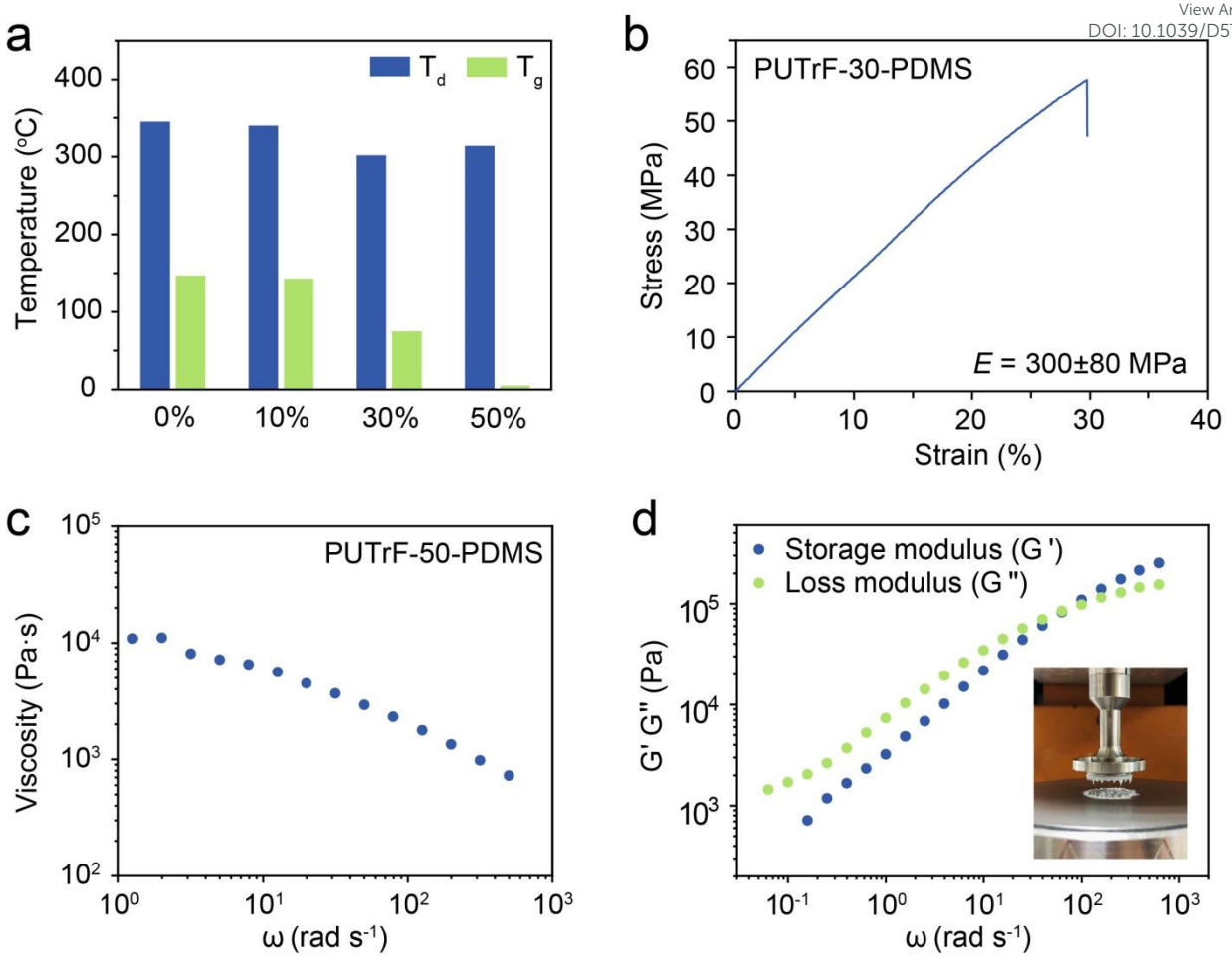

Fig. 3 (a) The decomposition temperature and glass transition temperature of PUTrF-co-PDMS. (b) Stress-strain curve of free-standing film of PUTrF-30-PDMS. (c) The shear sweep viscosity, as well as (d) storage modulus (G') and loss modulus (G'') versus angular velocity of PUTrF-50-PDMS in solid state. The inset shows the copolymer in testing.

For copolymers with 30% and 50% PDMS incorporating, they exhibited a melting peak around 210°C. These results clearly demonstrate that the introduction of soft segments enhances polymer chain mobility and increases free volume, thereby reducing the activation energy required for chain segment motion. However, due to the inherent brittleness of these copolymers at low soft-to-rigid ratios, both PUTrF and PUTrF-10-PDMS could not be fabricated into free-standing films for tensile testing. Consequently, quantitative mechanical characterization via tensile testing was conducted for PUTrF-30-PDMS. Figure 3b reveals that PUTrF-30-PDMS achieves an elongation at break of 30% with an elastic modulus of 300±80 MPa. The modulus is comparable to the 173 MPa of block copolymers based on diketopyrrolopyrrole (DPP) and poly(ε-caprolactone) reported by F. Sugiyama and co-workers[15]. PUTrF-50-PDMS shows a cream-like viscous state at ambient temperature due to the high flexibility and segmental migration of the molecular chains, which prompted us to conduct rheological test. Figure 3c displays the shear sweep viscosity of this copolymer, which decreased in one order of magnitude (10^4 to 10^3 Pa·s) with increasing angular velocity (ω). One reason is that the molecular chains were gradually disentangled and oriented along the flow direction, and the other reason is that the hydrogen bonds were broken under strong shear force, leading to weakened intermolecular interactions. Additionally, the storage modulus (G') and loss modulus (G") shown in Figure 3d reveals that, PUTrF-50-PDMS appears as a viscous state (G' < G") at low shear rate (< 62 rad/s), owing to the dissipation of soft segments plays a dominant role. On the contrary, the copolymer appears as an elastic state (G' > G) at high shear rate (> 62 rad/s), attributable to the predominance of dynamically reversible hydrogen-bonded interchain crosslinks that effectively suppressed extensive polymer chain slippage under rapid shear conditions. This phenomenon was consistent to the time-temperature superposition rheological master curves at the reference temperature of 20°C that performed on PUTrF-50-PDMS (Figure S10). These results demonstrate that constructing copolymers by combining chain segment of elastomers and interchain non-covalent interactions is a practical strategy for tuning the mechanical properties of polymers tailored for stretchable electronics.

Solution processability of these copolymers

These copolymers exhibit good solubility in chlorobenzene (CB) solvent, forming optically transparent solutions upon heating. In contrast, PUTrF-30-PDMS and PUTrF-50-PDMS solutions in toluene remained turbidity even at elevated temperatures, which mainly resulted by the stronger hydrogen bonding

View Article Online
DOI: 10.1039/D5TC02016F

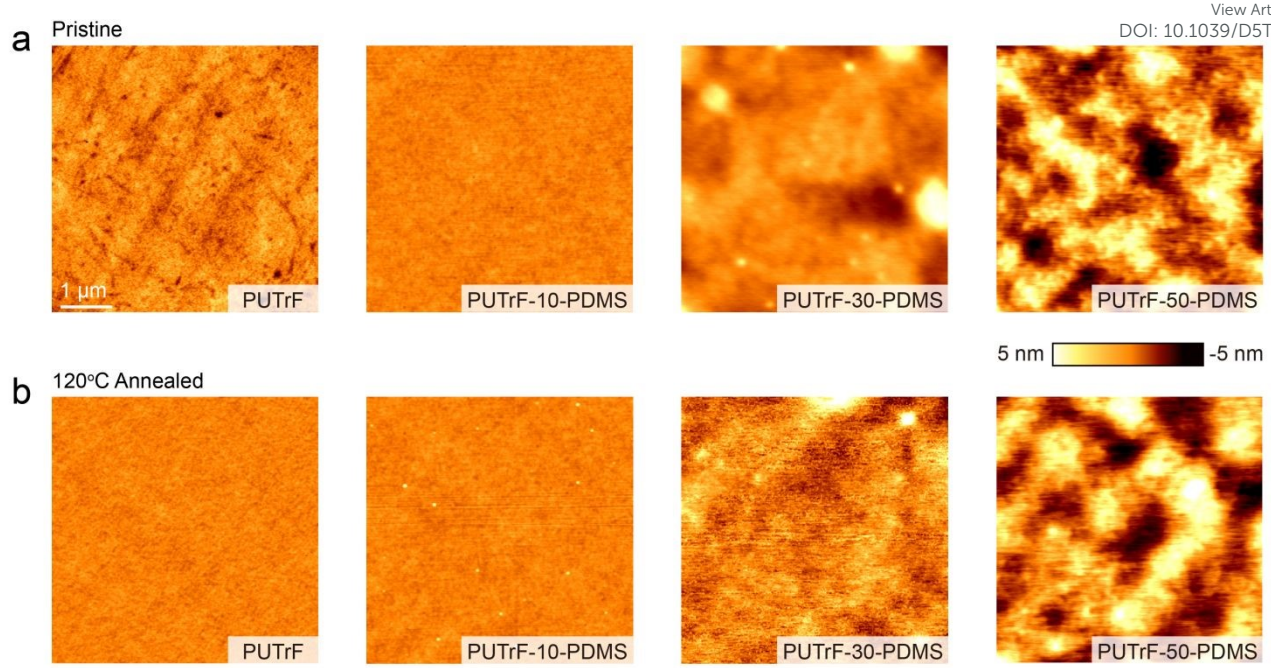

Fig. 4. Morphology characterization of solution-processed films. AFM height images of (a) the pristine spin-coated films and (b) thermal annealed films of these copolymers, tested in taping-mode with scan size of 5×5 μm. Thermal annealed condition: 120°C for 15 min under N_2 atmosphere.

facilitated by decreased polymer chain flexibility. Thus, we selected CB as the solvent for solution processing, and characterized their film morphologies and stacking structures by employing atomic force microscopy (AFM) and grazing incidence X-ray diffraction (GI-XRD). Figure 4 displays the height images of solution-processed films before and after thermal annealing. It can be observed that films of PUTrF and PUTrF-10-PDMS exhibit an extremely smooth and flat surface with root-mean-square roughness (R_q) below 0.5 nm, indicating the proportion of PDMS has not yet significantly disrupted the film uniformity. However, as the proportion of PDMS increased from 30% to 50%, microscopic phase separation emerged and became more pronounced in the film of PUTrF-50-PDMS. As shown in Figure S11, the phase image of this copolymer film presents an "island-like" topography, where the separated “island” corresponds to the domain of rigid segment and the continuous “ocean” represents the flat region of soft segment. This microscopic phase separation is primarily driven by the interfacial energy difference between soft and rigid segments during film formation, that the rigid chains self-assembled into densely packed domains due to reduced chain mobility and lower volumetric shrinkage. Additionally, the surface morphologies of these films kept stable after thermal annealing, indicating the good thermal stability of these copolymers during device fabrication (Figure 4b). From the 2D patterns of GI-XRD shown in Figure S12, no sharp diffraction rings and spots appeared in these solution-processed films, indicating the amorphous state of them. All of these results above demonstrate that the soft-to-rigid segment ratio significantly influences the morphological evolution of solution-processed films, which will have great impact on the devices’ performances.

Optical spectra and PLEDs characterization

Photophysical properties of these copolymers in film state were investigated. The maximum absorption peak of all these copolymers is located at 359 nm due to they possess identical conjugated units (Figure S13). Moreover, all the films exhibited deep-blue emission with peaks located at 403 nm and 425 nm, corresponding to 0-0 and 0-1 vibronic transitions, respectively (Figure 5a). The consistent optical spectra indicates that the ratio of soft-to-rigid segments have negligible influence on the photophysical properties of diarylfluorene trimer. The solution-processed films exhibited photoluminescence quantum yields (PLQY) of approximately 30%, comparable to that of blue light-emitting conjugated polymers, demonstrating the stability in radiative recombination efficiency despite structural modifications (Figure S14). In addition, the photoluminescence (PL) lifetime of these films were measured (Figure S15), and all copolymers exhibited single-exponential decay curves with lifetime values about 0.4 ns, confirming that the dominant singlet exciton behavior have not been affected in these novel copolymers.

Ultimately, polymer light-emitting diodes (PLEDs) were fabricated in order to investigate the electroluminescent (EL) properties of these copolymers. Figure 5b displays the device structure and energy level diagram of the functional layers, where the spin-coated copolymer films were adopted as the emitting layer (EML). The energy levels of the highest occupied molecular orbital (HOMO) of them were determined by cyclic voltammetry (CV) measurements. As shown in Figure S16, the HOMO energy levels of PUTrF-co-PDMS remain almost unchanged (-5.8 eV) across the PDMS ratio ranging from 0 to 30%. However, when the ratio increased to 50%, the HOMO energy level deepened significantly to -6.5 eV, creating a substantial energy barrier for hole injection into the EML and

View Article Online
DOI: 10.1039/D5TC02016F

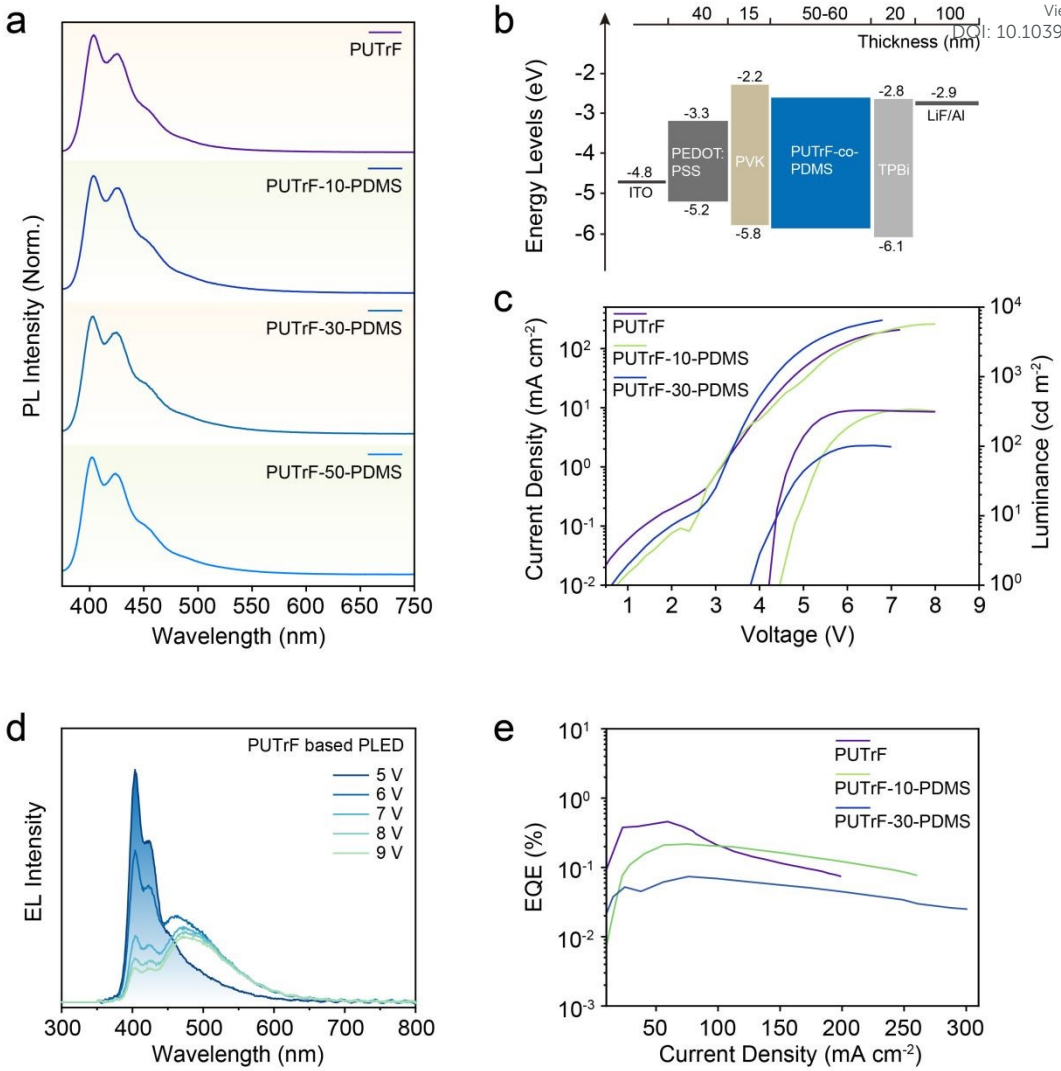

Fig. 5. (a) PL spectra of PUTrF-co-PDMS spin-coated films. (b) Energy level diagram of PLEDs. (c) Current density-Voltage-Luminance characteristic curves of the PLEDs. (d) EL spectra of PUTrF-based PLED at different voltages. (e) EQE-Current density curves of PLEDs based on PUTrF-co-PDMS films.

consequently impairing the charge recombination efficiency. That is why the PLED device based on PUTrF-50-PDMS failed to operate under the same condition. From the current density-voltage-luminance (*J-V-L*) curves depicted in Figure 5c, it can be observed that the turn-on voltages (V_{on}) of PLEDs based on the other three copolymers are around 4 V, comparable to those of polyfluorene-based blue PLEDs.[28] However, owing to the non-conjugated soft chains inevitably trap the charges and impede exciton recombination, the maximum luminescence of devices based on PUTrF and PUTrF-10-PDMS can only reach 436 and 439 cd/m², while the maximum luminescence of device based on PUTrF-30-PDMS is drastically reduced to 103 cd/m². Furthermore, the voltage-dependent EL spectra in Figures 5d and S17 reveal that these devices initially exhibit deep-blue emission with peaks at 404 and 423 nm, while an green emission (> 468 nm) emerges prominently at applied voltages above 7 V. The undesirable emission primarily originates from low-energy defect states induced by interchain aggregation.[29,30] The maximum external quantum efficiency (EQE) values of devices based on these novel copolymers are 0.6% for PUTrF, 0.7% for PUTrF-10-PDMS (Figure 5e). Nevertheless, the EQE of the device based on PUTrF-30-PDMS sharply decreased to 0.07%. In order to investigate the carrier transport ability of these copolymers, we fabricated single-charge-carrier devices. The average hole and electron mobility calculated by space-charge limited current (SCLC) method were shown in Figure S18-S20. We observed that, the hole mobility of these polymers showed gradually decrease as the ratio of PDMS increased from 0% to 50%. However, the electron mobility exhibited a non-monotonic dependence on PDMS ratio, the average value increased initially as the ratio of PDMS increased from 0% to 30%, then reduced drastically at 50% ratio. Therefore, we attribute the failure of device based on PUTrF-50-PDMS to the significantly reduced carrier mobility, with both hole and electron mobility being severely compromised at this content. As for the dropped EQE observed in devices based on other copolymers, we speculate it was the result of a combination of multiple factors, including the imbalanced carrier mobility and increased morphological heterogeneity. Thus, constructing stretchable emitting layer without sacrificing the devices'

performances still remains huge challenges. It's urgent to explore effective approaches for achieving an optimal balance between mechanical and optoelectronic properties in these block copolymers.

Conclusions

In this study, by incorporating diarylfluorene-based trimer (rigid segments) and PDMS (soft segments) through polycondensation for fabricating PU, we reported a series of blue light-emitting copolymers with tunable mechanical properties. By varying the ratio of soft-to-rigid segments (0-50%), these copolymers transitioned from brittle solid to viscoelastic materials with T_g reduced from 147°C to 5°C. The interchain hydrogen bonding formed by urethane groups contributed to shear-thinning behavior (10^{-4} to 10^{-3} Pa·s) and elastic-viscous transition. The solution-processed films of these copolymers maintained deep-blue emission with a PLQY of ~30%. In addition, PLEDs based on some of these copolymers were successfully fabricated, and the turn-on voltages (~4 V) were comparable to the reported blue PLEDs. However, due to the charge trapping and aggregation-induced defects, these devices showed limited luminance (< 440 cd/m^2) and unsatisfactory EL spectra stability. Our work provides a feasible strategy for designing stretchable light-emitting polymers and highlights the importance of balancing the mechanical and optoelectronic performances for flexible optoelectronics.

Author contributions

Xinyu Liang: Writing-original draft, Visualization, Investigation. Wenxin Huang: Investigation, Data curation. Rui Gao: Investigation, Data curation. Qingqing Lu: Investigation, Data curation. Mengyuan Li: Investigation, Data curation. Zhiqiang Zhuo: Investigation, Data curation. Mingjian Ni: Investigation, Data curation. Ning Sun: Investigation, Data curation. Lili Sun: Investigation, Data curation. Xiang An: Investigation, Data curation. Yamin Han: Writing-review & editing. Jinyi Lin: Funding acquisition, Supervision. Lubing Bai: Conceptualization, Methodology, Funding acquisition.

Data availability

The data supporting this article have been included as part of the ESI.†

Conflicts of interest

There are no conflicts to declare.

Acknowledgements

This work was supported by the National Natural Science Foundation of China (62105262, 62205141, 22075136, 62405134), the Natural Science Funds of the Education Committee of Jiangsu Province (23KJA430010), the Natural Science Foundation of Jiangsu Province for Youth (BK20230342), the China Postdoctoral Science Foundation (2024M753737), the Shenzhen Science and Technology Program (RCBS20231211090610014), the open research fund from the Key Laboratory of Advanced Display and System Applications, Ministry of Education, Shanghai University (OF202505), the Cultivation Program for the Excellent Doctoral Dissertation of Nanjing Tech University (2024-15), the Postgraduate Research & Practice Innovation Program of Jiangsu Province (KYCX25-1710).

References

1 Y. Lee, H. Cho, H. Yoon, H. Kang, H. Yoo, H. Zhou, S. Jeong, G. H. Lee, G. Kim, G. T. Go, J. Seo, T. W. Lee, Y. Hong and Y. Yun, *Adv. Mater. Technol*. 2023, **8**, 2201067.
2 Z. Zhang, Y. Wang, S. Jia and C. Fan, *Nat. Photon*. 2024, **18**, 114-126.
3 H. Yin, Y. Zhu, K. Youssef, Z. Yu and Q. Pei, *Adv. Mater*. 2021, **34**, 2106184.
4 K. Keum, S. Yang, K. S. Kim, S. K. Park and Y.-H. Kim, *Soft Sci*. 2024, **4**, 34.
5 Z. Zhang, W. Wang, Y. Jiang, Y.-X. Wang, Y. Wu, J.-C. Lai, S. Niu, C. Xu, C.-C. Shih, C. Wang, H. Yan, L. Galuska, N. Prine, H.-C. Wu, D. Zhong, G. Chen, N. Matsuhisa, Y. Zheng, Z. Yu, Y. Wang, R. Dauskardt, X. Gu, J. B. H. Tok and Z. Bao, *Nature* 2022, **603**, 624-630.
6 A. Shinohara, C. Pan, Z. Guo, L. Zhou, Z. Liu, L. Du, Z. Yan, F. J. Stadler, L. Wang and T. Nakanishi, *Angew. Chem. Int. Ed.* 2019, **58**, 9581-9585.
7 Z. Guo, A. Shinohara, C. Pan, F. J. Stadler, Z. Liu, Z.-C. Yan, J. Zhao, L. Wang and T. Nakanishi, *Mater. Horiz*. 2020, **7**, 1421-1426.
8 A. Tateyama, K. Nagura, M. Yamanaka and T. Nakanishi, *Angew. Chem. Int. Ed.* 2024, **63**, 2402874.
9 X. An, H. Gong, W. Chen, Z. Zhuo, C. Wei, N. Sun, M. Ni, B. Liu, J. Wang, L. Bai, P. Sun, J. Lin and W. Huang, *Adv. Optical Mater.* 2024, **12**, 2400010.
10 Y. Zhao, X. Zhao, M. Roders, A. Gumyusenge, A. L. Ayzner and J. Mei, *Adv. Mater*. 2017, **29**, 1605056.
11 D. Pei, B. Zhao, C. An, Y. Guo, K. Zhou, Y. Deng, Y. Han and Y. Geng, *Macromolecules* 2024, **57**, 3138-3147.
12 S. Seo, J. W. Lee, D. J. Kim, D. Lee, T. N. Phan, J. Park, Z. Tan, S. Cho, T. S. Kim and B. J. Kim, *Adv. Mater*. 2023, **35**, 2300230.
13 D. Pei, C. An, B. Zhao, M. Ge, Z. Wang, W. Dong, C. Wang, Y. Deng, D. Song, Z. Ma, Y. Han and Y. Geng, *ACS Appl. Mater. Interfaces*. 2022, **14**, 33806-33816.
14 A.-N. Au-Duong, C.-C. Wu, Y.-T. Li, Y.-S. Huang, H.-Y. Cai, I. Jo Hai, Y.-H. Cheng, C.-C. Hu, J.-Y. Lai, C.-C. Kuo and Y.-C. Chiu, *Macromolecules* 2020, **53**, 4030-4037.
15 F. Sugiyama, A. T. Kleinschmidt, L. V. Kayser, M. A. Alkhadra, J. M. H. Wan, A. S. C. Chiang, D. Rodriquez, S. E. Root, S. Savagatrup and D. J. Lipomi, *Macromolecules* 2018, **51**, 5944-5949.
16 X. Chen, J. Zhou, Z. Xie and Y. Ma, *Info & Funct. Mater*. 2024, **1**, 68-86.
17 S. Fratini, M. Nikolka, A. Salleo, G. Schweicher and H. Sirringhaus, *Nat. Mater.* 2020, **19**, 491-502.
18 M. W. Jeong, J. H. Ma, J. S. Shin, J. S. Kim, G. Ma, T. U. Nam, X. Gu, S. J. Kang and J. Y. Oh, *Sci. Adv.* 2023, *9*, eadh1504.
19 K.-H. Jeon and J.-W. Park, *Macromolecules* 2022, **55**, 8311-8320.
20 L. Janasz, M. Borkowski, P. W. M. Blom, T. Marszalek and W. Pisula, *Adv. Funct. Mater*. 2021, **32**, 2105456.

View Article Online
DOI: 10.1039/D5TC02016F

21 J. Xu, S. Wang, G.-J. N. Wang, C. Zhu, S. Luo, L. Jin, X. Gu, S. Chen, V. R. Feig, J. W. F. To, S. Rondeau-Gagné, J. Park, B. C. Schroeder, C. Lu, J. Y. Oh, Y. Wang, Y.-H. Kim, H. Yan, R. Sinclair, D. Zhou, G. Xue, B. Murmann, C. Linder, W. Cai, J. B.-H. Tok, J. W. Chung and Z. Bao, *Science* 2017, **355**, 59-64.
22 Y.-S. Guan, F. Ershad, Z. Rao, Z. Ke, E. C. da Costa, Q. Xiang, Y. Lu, X. Wang, J. Mei, P. Vanderslice, C. Hochman-Mendez and C. Yu, *Nat. Electron*. 2022, **5**, 881-892.
23 S. Li, M. Gao, K. Zhou, X. Li, K. Xian, W. Zhao, Y. Chen, C. He and L. Ye, *Adv. Mater*. 2023, **36**, e2307278.
24 W. Yang, X. Luo, M. Li, C. Shi, Z. Wang, Z. Yang, J. Wu, X. Zhang, W. Huang, D. Ma, C. Wang, W. Zhong and L. Ying, *Adv. Energy. Mater*. 2024, **15**, 2403259.
25 J. Kang, D. Son, G. N. Wang, Y. Liu, J. Lopez, Y. Kim, J. Y. Oh, T. Katsumata, J. Mun, Y. Lee, L. Jin, J. B. Tok and Z. Bao, *Adv. Mater*. 2018, **30**, 1706846.
26 W. Yao, X. Sui, D. Yang, X. Hu, J. Huang, Q. Tian and X. Liu, *Adv. Funct. Mater*. 2023, **34**, 2313842.
27 Y. Zheng, M. Ashizawa, S. Zhang, J. Kang, S. Nikzad, Z. Yu, Y. Ochiai, H.-C. Wu, H. Tran, J. Mun, Y.-Q. Zheng, J. B. H. Tok, X. Gu and Z. Bao, *Chem. Mater*. 2020, **32**, 5700-5714.
28 H. Gong, W. Huang, W. Chen, L.-B. Bai, X. Liang, Y. Zheng, Q. Lu, R. Gao, Y. Han, Z. Zhuo, X. An, J.-Y. Lin and W. Huang, *Poly. Chem*. 2024, **15**, 3176-3183.
29 T. Nakamura, D. K. Sharma, S. Hirata and M. Vacha, *J. Phys. Chem. C* 2018, **122**, 8137-8146.
30 M. Sims, D. D. C. Bradley, M. Ariu, M. Koeberg, A. Asimakis, M. Grell and D. G. Lidzey, *Adv. Funct. Mater*. 2004, **14**, 765-781.

View Article Online
DOI: 10.1039/D5TC02016F

Balancing the Mechanical and Optoelectronic Properties of Light-Emitting Copolymers via Precise Control of Soft-to-Rigid Segment Ratio

Xinyu Liang,‡[a] Wenxin Huang,‡[a] Qingqing Lu,‡[a] Rui Gao,[a] Mengyuan Li,[a] Zhiqiang Zhuo,[a] Mingjian Ni,[b] Ning Sun,[a] Lili Sun,[c] Xiang An,[a] Yamin Han,[a] Jinyi Lin[a] and Lubing Bai*[a]

Data availability

The data supporting this article have been included as part of the ESI.†